

# Decay of zone-center phonons in GaN with $A_1$ , $E_1$ , and $E_2$ symmetries

D. Y. Song, S. A. Nikishin, and M. Holtz<sup>a)</sup>  
Texas Tech University, Lubbock, Texas 79409

V. Soukhovveev, A. Usikov, and V. Dmitriev  
TDI, Inc., 12214 Plum Orchard Drive, Silver Spring, Maryland 20904

(Received 28 October 2006; accepted 11 December 2006; published online 15 March 2007)

We report Raman studies of the  $A_1(\text{TO})$ ,  $E_1(\text{TO})$ ,  $E_2^2$ ,  $A_1(\text{LO})$ , and  $E_1(\text{LO})$  symmetry phonons of GaN from 20 to 325 K. By applying anharmonic decay theory to the observed temperature dependences of the phonon energies and linewidths, we determine the phonon decay mechanisms of these zone-center vibrations. Thermal expansion is taken into account using published temperature-dependent coefficients. The  $A_1(\text{TO})$  and  $E_1(\text{TO})$  vibrations are described by symmetric two-phonon decay. The  $E_2^2$  decays via the creation of three phonons. Both  $A_1(\text{LO})$  and  $E_1(\text{LO})$  bands are interpreted by an asymmetric two-phonon decay, with a minor contribution to the decay of the former from the three-phonon creation. Phonon lifetimes are obtained based on the observed linewidths. © 2007 American Institute of Physics. [DOI: 10.1063/1.2561930]

## I. INTRODUCTION

Self-heating in optoelectronic and electronic devices is a substantial problem in situations with high current density. This is particularly important where current crowding takes place through miniaturization or in devices based on two-dimensional electron gases.<sup>1–3</sup> Self-heating degrades performance and is an important failure mechanism. In polar materials, such as AlGaIn, hot electron energy is dissipated predominantly through Fröhlich electron-phonon scattering. Due to the form of the Fröhlich interaction, phonons produced by this carrier relaxation process are primarily zone-center longitudinal-optical (LO) vibrations.<sup>4</sup> Because the LO phonons behave like standing waves, they must decay into traveling acoustic waves to dissipate energy from the immediate self-heating region. Understanding of the intrinsic phonon decay properties of high-quality crystalline materials is thus critical to self-heating and any phonon engineering efforts to mitigate the associated device problems.

Owing to the  $\mathbf{q}=0$  selection rule, where  $\mathbf{q}$  is the wave vector, Raman scattering is ideally suited for studying the phonons which are important for carrier relaxation in polar semiconductors. One approach to lifetime studies is through measurements of Raman linewidths ( $\Gamma$ ) which are inversely proportional to the overall phonon lifetime ( $\tau_{\text{total}}$ ). In general,<sup>5</sup> the phonon lifetime is influenced by anharmonic decay and inhomogeneous impurity phonon scattering according to

$$2\pi c\Gamma = \frac{1}{\tau_{\text{total}}} = \frac{1}{\tau_{\text{decay}}} + \frac{1}{\tau_i}, \quad (1)$$

where  $c$  is the speed of light in vacuum in cm/s and  $\Gamma$  is in  $\text{cm}^{-1}$ . The average phonon decay time is  $\tau_{\text{decay}}$ , while  $\tau_i$  represents the effect of all impurity and defect scattering processes limiting the lifetime. The latter is generally taken to

be small, corresponding to high-quality crystals, and temperature independent. When impurity scattering is negligible in comparison to the anharmonic processes, direct measurement of  $\Gamma$  can be used to obtain the decay time  $\tau_{\text{decay}}$ .

Fundamentally, phonons may decay into two or more lower energy vibrations, provided total energy and wave vector are each conserved according to

$$\omega = \sum_{i=1}^N \omega_i, \quad (2a)$$

$$\mathbf{q} = \sum_{i=1}^N \mathbf{q}_i + \mathbf{G}, \quad (2b)$$

respectively, where  $\omega(\omega_i)$  represents initial (created) phonon energy (in  $\text{cm}^{-1}$ ),  $\mathbf{q}(\mathbf{q}_i)$  the initial (created) phonon wave vector, and  $\mathbf{G}$  is a reciprocal lattice vector.  $N$  is the number of phonons created in the decay process. Phonon decay channels producing vibrations with high density of states contribute most strongly to the process, and lower order processes have higher probability when they satisfy the above stipulations. In the current context, it is the phonon joint density of states that is relevant, which must be calculated subject to constraint [Eq. (2b)]. For two-phonon decay, the corresponding joint density of states has been reported in Ref. 6.

The prevailing two-phonon decay mechanisms are referred to as Klemens<sup>7</sup> and Ridley<sup>8</sup> processes. In the Klemens process an optical phonon decays into two identical acoustic phonons with opposite momenta. The decay of one LO phonon into one transverse-optical (TO) phonon and one longitudinal-acoustic (LA) phonon is known as the Ridley channel. The Ridley channel is relevant when large energy differences exist between optic and acoustic branches caused by the large differences in anion and cation masses. The two-phonon process does not fully describe the phonon decay mechanism in all cases. Under these circumstances, it is usual to include third- or higher-order phonon decay processes.

<sup>a)</sup>Author to whom correspondence should be addressed; electronic mail: mark.holtz@ttu.edu

Temperature-dependent Raman scattering measurements are widely used for examining zone-center phonon decay processes in high-quality crystals. Both the phonon energy and the linewidth may be accurately described according to the phonon decay model. Previous reports concerning phonon decay have used Raman scattering to examine the  $E_2^2$  and  $A_1(\text{LO})$  phonon decay properties in GaN (Refs. 9–11) since these phonons are allowed in the (0001) backscattering configuration and are therefore readily measurable. We find only one paper reporting decay properties of zone-center phonons other than  $A_1(\text{LO})$  and  $E_2^2$ .<sup>12</sup> However, this paper addresses decay using only symmetric processes, an approach which is not generally accepted particularly for the  $A_1(\text{LO})$  phonon, which is believed to decay according to the Ridley process.<sup>8,10,11</sup> In the current paper, we report studies of the  $A_1(\text{TO})$ ,  $E_1(\text{TO})$ ,  $E_2^2$ ,  $A_1(\text{LO})$ , and  $E_1(\text{LO})$  phonons in epitaxial GaN and we examine their decay properties based on anharmonic theory.

## II. PHONON DECAY

Menendez and Cardona treated phonon decay in nonpolar Si and Ge and derived expressions for energy shift and broadening when two and three phonons are created.<sup>13</sup> The situation for polar materials has been examined by Debernardi.<sup>14,15</sup> The phonon population at thermal equilibrium is described by the Bose-Einstein function  $n_j(\mathbf{q}) = [\exp(\hbar c \omega_j(\mathbf{q})/k_B T) - 1]^{-1}$  at energy  $\hbar c \omega_j$ , where  $j$  denotes the phonon branch and  $\omega_j$  is in  $\text{cm}^{-1}$ . Within the single-mode relaxation time approach,<sup>15</sup> the initial phonon at  $\mathbf{q}=\mathbf{0}$  has a nonequilibrium population and phonons at all other points of the Brillouin zone are assumed to be in equilibrium. In our experiments, the nonequilibrium abundance of  $\mathbf{q}=\mathbf{0}$  phonons arises from the Raman process. The decay-related broadening is<sup>14,16</sup>

$$\begin{aligned} \Gamma(\mathbf{0}, j; \omega) = & \frac{18\pi}{\hbar^2} \sum_{\mathbf{q}_1, j_1, j_2} |V_3|^2 \times [n_{j_1}(\mathbf{q}) + n_{j_2}(-\mathbf{q}) + 1] \\ & \times \delta[\omega(\mathbf{0}) - \omega_{j_1}(\mathbf{q}) - \omega_{j_2}(-\mathbf{q})] \\ & + \frac{96\pi}{\hbar^2} \sum_{\mathbf{q}_1, \mathbf{q}_2, \mathbf{q}_3, j_1, j_2, j_3} |V_4|^2 \times \{[n_{j_1}(\mathbf{q}_1) + 1] \\ & \times [n_{j_2}(\mathbf{q}_2) + 1][n_{j_3}(\mathbf{q}_3) + 1] \\ & - n_{j_1}(\mathbf{q}_1)n_{j_2}(\mathbf{q}_2)n_{j_3}(\mathbf{q}_3)\} \times \delta[\omega(\mathbf{0}) - \omega_{j_1}(\mathbf{q}_1) \\ & - \omega_{j_2}(\mathbf{q}_2) - \omega_{j_3}(\mathbf{q}_3)], \end{aligned} \quad (3)$$

where the Dirac  $\delta$  functions in Eq. (3) originate from density of states arguments and ensures conservation of energy (explicit) and wave vector (implicit) in allowed transitions.<sup>17,18</sup> The first term in Eq. (3) originates from the third-order anharmonic factor of the vibrational Hamiltonian and describes the decay of one phonon at the zone center into two phonons with opposite wave vectors (two-phonon decay). The second term in Eq. (3) arises from the fourth-order expansion factor in the vibrational Hamiltonian and corresponds to the decay of one phonon at the zone center into three phonons under the Eq. (2b) constraint  $\mathbf{q}_1 + \mathbf{q}_2 + \mathbf{q}_3 = \mathbf{0}$  (three-phonon decay).

The matrix elements  $V_3$  and  $V_4$  are related to the Fourier-transformed cubic and quartic anharmonic force constants (see, e.g., Refs. 14 and 19).

The phonon energy shift induced solely by anharmonic decay can be expressed through the Kramers-Kronig transform of  $\Gamma(\mathbf{0}, j, \omega)$  (Refs. 15 and 18),

$$\Delta(\mathbf{0}, j, \omega) = -\frac{2}{\pi} P \int_0^\infty \frac{\omega' \Gamma(\mathbf{0}, j, \omega')}{(\omega'^2 - \omega^2)} d\omega', \quad (4)$$

where  $P$  denotes the principal part of the integral.

The heavily constrained situation described by each term in Eq. (3) results in phonon decay processes involving only a few vibrations from within the Brillouin zone. In situations where two- and three-phonon decay processes may be attributed to a single (or narrow) set of created phonons, each sum in Eq. (3) may be replaced by a single term. In this case, we may introduce simplified parameters  $A$  and  $B$  as coefficients of two- and three-phonon decay processes in Eq. (4). Considering the lowest order anharmonic (thermal expansion) contribution, the temperature dependence of the phonon energy  $\omega(T)$  can be written as<sup>13,18</sup>

$$\begin{aligned} \omega(T) = & \omega_0 + \Delta_0(T) + A(1 + n_1 + n_2) + B(1 + n_3 + n_4 + n_5 \\ & + n_3 n_4 + n_3 n_5 + n_4 n_5), \end{aligned} \quad (5)$$

where  $\omega_0$  is the harmonic frequency of the phonon mode and  $\Delta_0(T)$  is the thermal expansion contribution to the frequency. Explicit temperature dependences of the Bose functions have been suppressed. The thermal expansion contribution is given by  $\Delta_0(T) = -\omega_0 \gamma \int_0^T [\alpha_c(T') + 2\alpha_a(T')] dT'$ , where  $\gamma$  is the Gruneisen parameter, and  $\alpha_c$  and  $\alpha_a$  are the linear thermal expansion coefficients parallel and perpendicular to the hexagonal  $c$  axis, respectively.<sup>9</sup> Recent work points out that the temperature dependence of the thermal expansion coefficients is important to take into account when examining the decay processes in GaN (Ref. 11) and AlN (Ref. 20). Using published values for  $\alpha_c$  and  $\alpha_a$  (Ref. 21) and for  $\gamma$ ,<sup>12</sup>  $\Delta_0(T)$  may be calculated with no fitting parameters.

For Raman lines which are symmetric the width is approximated by  $2\Gamma(\mathbf{0}, j, \omega)$  in Eq. (3).<sup>15</sup> Introducing analogously simplified parameters  $C$  and  $D$  as coefficients of two- and three-phonon decays in Eq. (3), the temperature dependence Raman linewidth  $\Gamma(T)$  is

$$\begin{aligned} \Gamma(T) = & \Gamma_0 + 2C(1 + n_1 + n_2) + 2D(1 + n_3 + n_4 + n_5 + n_3 n_4 \\ & + n_3 n_5 + n_4 n_5), \end{aligned} \quad (6)$$

where  $\Gamma_0 + 2C + 2D$  is the  $T \rightarrow 0$  phonon linewidth. In this paper we use Eqs. (5) and (6) to fit the temperature dependences for the respective Raman bands. By fitting both phonon energy and linewidth dependences, we obtain a detailed picture of the decay processes involved for each GaN phonon studied.

## III. EXPERIMENTAL DETAILS

The nominally undoped GaN layers, with thickness  $\sim 80 \mu\text{m}$ , were grown using hydride vapor phase epitaxy on 50 mm sapphire substrates. The concentration of electrically active (noncompensated) donors was in the  $10^{16} \text{ cm}^{-3}$  range.

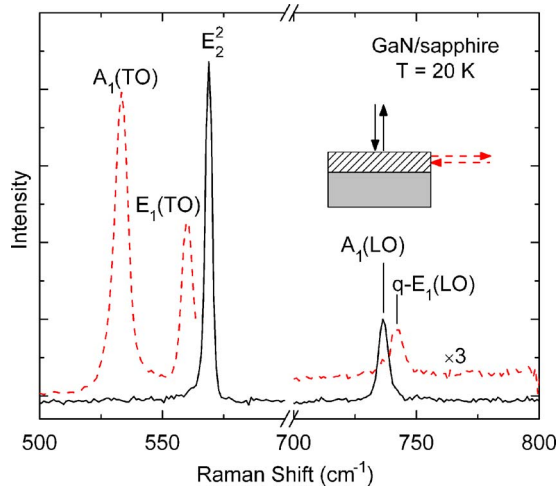


FIG. 1. (Color online) Typical Raman spectra of GaN observed at different scattering geometries at  $T=20$  K. The solid curve is for backscattering along the (0001) crystal growth axis, the dashed curve is for backscattering from the epilayer edge (see inset).

X-ray diffraction reveals layers to have low dislocation density,  $\sim 10^8$   $\text{cm}^{-2}$ , and to be strain relaxed with in-plane strains  $< 0.06\%$ .<sup>11</sup> This material exhibits narrow Raman bands allowing investigation of the linewidths and implications for phonon lifetime.

Micro-Raman measurements were obtained in the backscattering geometry from the standard  $c$  plane, for which the  $E_2^2$  and  $A_1(\text{LO})$  phonons are allowed. In order to examine phonons with the  $E_1$  symmetry and the  $A_1(\text{TO})$  band, the

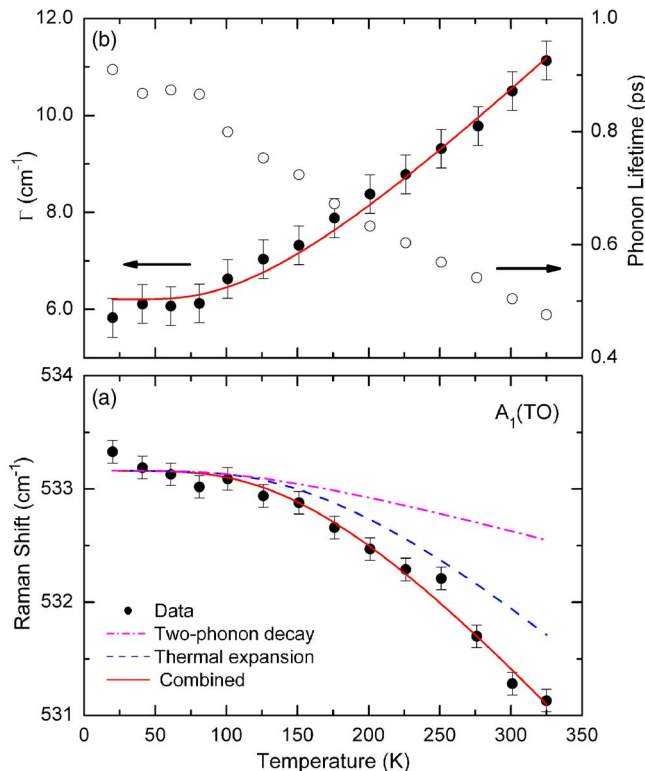


FIG. 2. (Color online) Dependence of  $A_1(\text{TO})$  phonon energies (a) and linewidths (b) on temperature. Curves are theory-based fits to data. Contributions of thermal expansion and phonon decay to the overall shifts are plotted separately. Phonon lifetime versus temperature is shown (b).

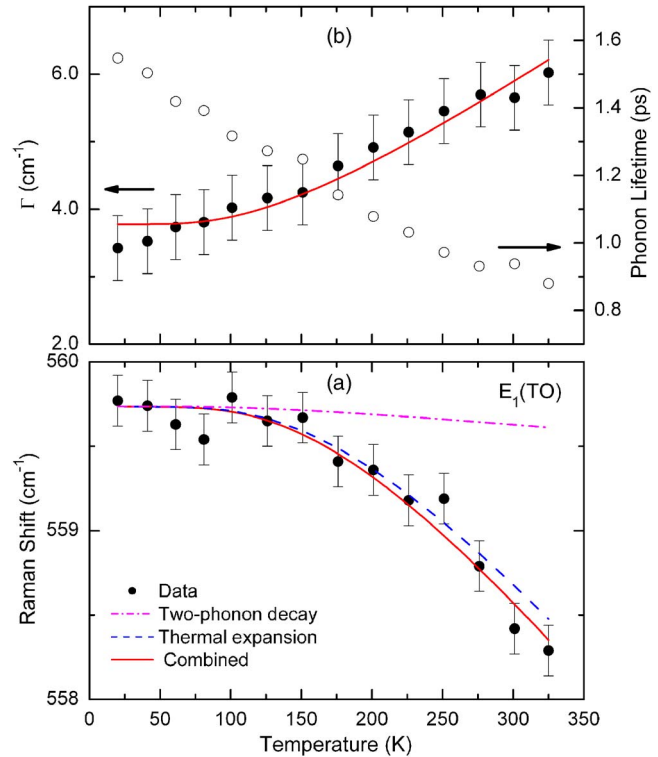


FIG. 3. (Color online) Dependence of  $E_1(\text{TO})$  phonon energies (a) and linewidths (b) on temperature, similar to Fig. 2.

crystal was cleaved and micro-Raman backscattering measurements were carried out from the cross-section surfaces with focus ( $\sim 2$   $\mu\text{m}$  probe diameter) close to the surface. Visible 488.0 nm excitation was used and the sample temperature controlled using a closed-cycle cryostat.<sup>22</sup> Representative spectra at low temperature are shown in Fig. 1. Raman peaks were fitted using a Lorentzian line shape; the reported linewidths are corrected for the 2.6  $\text{cm}^{-1}$  instrumental bandpass of the Raman system.

#### IV. $A_1(\text{TO})$ , $E_1(\text{TO})$ , AND $E_2^2$ PHONON DECAY

The phonon energies and linewidths of the  $A_1(\text{TO})$ ,  $E_1(\text{TO})$ , and  $E_2^2$  are shown as functions of temperature in Figs. 2–4, respectively. Also shown on the right-hand axes of all linewidth graphs are the phonon lifetimes obtained using Eq. (1). The  $A_1(\text{TO})$  and  $E_1(\text{TO})$  dependences exhibit similar dependences, while the  $E_2^2$  dependence is more gradual. In each case, we fit the energy shift dependence using Eq. (5) and the line broadening using Eq. (6). Fit results are summarized in Table I.

For the  $A_1(\text{TO})$  phonon we find  $\omega_1 = \omega_2 \sim 267$   $\text{cm}^{-1}$  corresponding to the symmetric Klemens channel. In Fig. 2(a), we also show the individual contributions of thermal expansion and phonon decay to the temperature shift. Thermal expansion accounts for  $\sim 2/3$  of the observed shift across the temperature range examined, illustrating the importance of correctly accounting for the thermal expansion effect. Temperature-induced broadening is significant for this phonon,  $\sim 5$   $\text{cm}^{-1}$  from 20 to 325 K. We analyze the temperature dependence of the  $A_1(\text{TO})$  broadening using the same values for  $\omega_1$  and  $\omega_2$  obtained from the phonon shift and fit

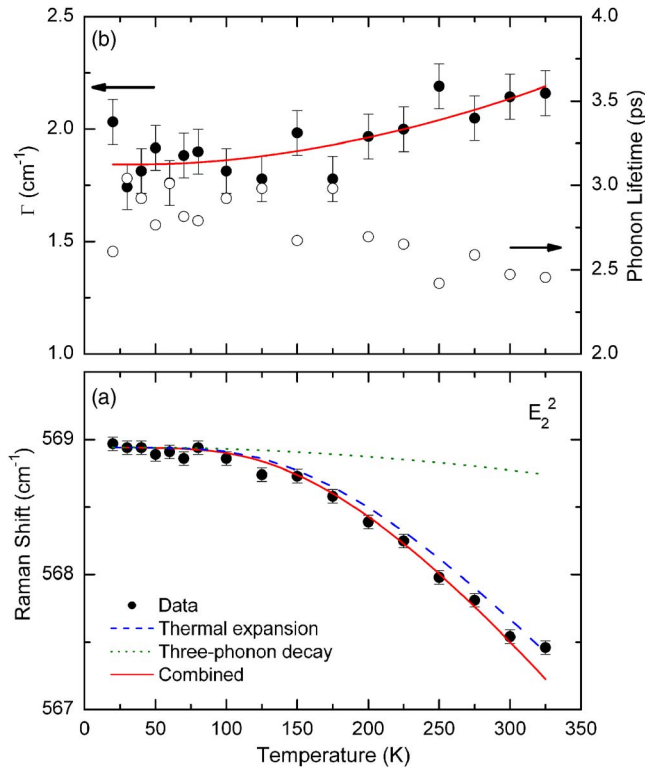


FIG. 4. (Color online) Dependence of  $E_2^2$  phonon energies (a) and linewidths (b) on temperature, similar to Fig. 2.

Eq. (6) to linewidth data varying parameters  $\Gamma_0$  and  $C$ , as shown by the solid curve in Fig. 2(b). The fit agrees well with the experimental data consistently showing the decay of  $A_1(\text{TO})$  into two phonons with identical energies. Examination of the GaN phonon dispersion curve<sup>23,24</sup> suggests two symmetric decay scenarios, the first producing two  $E_2^1$  phonons near the  $H$  symmetry point and the second creating acoustic phonons in the  $K$ - $M$  range of the Brillouin zone.

We similarly analyze the  $E_1(\text{TO})$  line as shown in Fig. 3. The shift is primarily attributed to the thermal expansion factor  $\Delta_0(T)$  and the linewidth broadens by  $\sim 2 \text{ cm}^{-1}$  over the temperature range studied. The  $E_1(\text{TO})$  phonon symmetrically decays via the creation of two phonons with energy of  $280 \text{ cm}^{-1}$ . Results are consistent for both the Raman shifts and the linewidths. An inspection of the phonon dispersion curve for GaN (Ref. 23) suggests that the decay produces  $E_1(\text{TO})$ -symmetry phonon into two  $B_1^1$  phonons from the  $K$  point of the Brillouin zone. We notice the change of the  $E_1(\text{TO})$  phonon linewidth remains smaller than the corresponding values of the  $A_1(\text{TO})$  band across the temperature range studied here. This indicates that the phonon decay process is weaker for the  $E_1(\text{TO})$  phonon, a conclusion that is confirmed by the smaller coefficient  $A$ . One possible explanation for this is a narrower range of phonons in the Brillouin zone participating in the  $E_1(\text{TO})$  decay process, although this is not reflected in the calculated two-phonon density of states which varies gradually across the  $520$ – $600 \text{ cm}^{-1}$  range.<sup>6</sup>

Unlike the  $E_1(\text{TO})$  phonon, both the energy and linewidth of the  $E_2^2$  band exhibit weak temperature dependences, redshifting by only  $\sim 1.5 \text{ cm}^{-1}$  and broadening  $\sim 0.5 \text{ cm}^{-1}$  across the temperature range studied (Fig. 4). The weak broadening is indicative of a higher-order decay mechanism. An analysis of the temperature dependence shows that the decay of  $E_2^2$  is not described by a two-phonon process. Rather, the  $E_2^2$  creates three acoustic phonons at  $\sim 190 \text{ cm}^{-1}$ . Regions of the Brillouin zone which may contribute to this decay process are phonons near the  $M$  and  $L$  symmetry points.

Both  $A_1(\text{TO})$  and  $E_1(\text{TO})$  phonons decay symmetrically into vibrations from the high density of state regions in the  $200$ – $300 \text{ cm}^{-1}$  range. In contrast to the LO phonons (discussed below), the two-phonon decay coefficients  $A$  obtained

TABLE I. Fitting results for Raman phonons. All  $T=0 \text{ K}$  values are from fits to the temperature dependences.

Symmetry	Energy	Linewidth
$A_1(\text{TO})$	$\omega_0=533.9 \text{ cm}^{-1}$ $A=0.69\pm 0.38 \text{ cm}^{-1}$ $B=0 \text{ cm}^{-1}$ $\omega_1=\omega_2=267.0 \text{ cm}^{-1}$	$\Gamma_0=0.55\pm 0.23 \text{ cm}^{-1}$ $2C=5.65\pm 0.19 \text{ cm}^{-1}$ , $2D=0$
$E_1(\text{TO})$	$\omega_0=560.0 \text{ cm}^{-1}$ $A=0.15\pm 0.10 \text{ cm}^{-1}$ , $B=0 \text{ cm}^{-1}$ $\omega_1=\omega_2=280.0 \text{ cm}^{-1}$	$\Gamma_0=0.8\pm 0.2 \text{ cm}^{-1}$ $2C=2.97\pm 0.19 \text{ cm}^{-1}$ , $2D=0$
$E_2^2$	$\omega_0=569.0 \text{ cm}^{-1}$ $A=0$ , $B=0.05\pm 0.01 \text{ cm}^{-1}$ $\omega_3=\omega_4=\omega_5=190.0 \text{ cm}^{-1}$	$\Gamma_0=1.76\pm 0.04 \text{ cm}^{-1}$ $2C=0$ , $2D=0.09\pm 0.02 \text{ cm}^{-1}$
$A_1(\text{LO})$	$\omega_0=738.3 \text{ cm}^{-1}$ $A=1.56\pm 0.08 \text{ cm}^{-1}$ $B=0.30\pm 0.02 \text{ cm}^{-1}$ $\omega_1=559.3 \text{ cm}^{-1}$ , $\omega_2=180 \text{ cm}^{-1}$ $\omega_3=\omega_4=\omega_5=246.1 \text{ cm}^{-1}$	$\Gamma_0=0.90\pm 0.16 \text{ cm}^{-1}$ $2C=2.06\pm 0.08 \text{ cm}^{-1}$ $2D=0.86\pm 0.06 \text{ cm}^{-1}$
$E_1(\text{LO})$	$\omega_0=745.0 \text{ cm}^{-1}$ $A=1.59\pm 0.16 \text{ cm}^{-1}$ , $B=0 \text{ cm}^{-1}$ $\omega_1=140.0 \text{ cm}^{-1}$ , $\omega_2=605.0 \text{ cm}^{-1}$	$\Gamma_0=3.28\pm 0.38 \text{ cm}^{-1}$ $2C=3.08\pm 0.24 \text{ cm}^{-1}$ , $2D=0 \text{ cm}^{-1}$

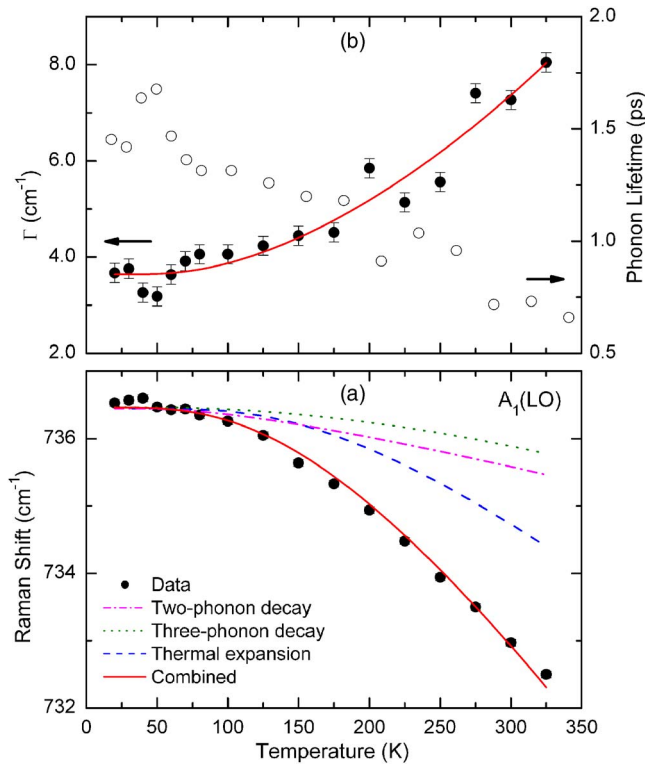


FIG. 5. (Color online) Dependence of  $A_1(\text{LO})$  phonon energies (a) and linewidths (b) on temperature, similar to Fig. 2.

from the energy shifts of the TO lines are much smaller than the  $C$  coefficients obtained from the linewidth analysis. A similar difference in fitting results was reported in Ref. 12. Published reports of the two-phonon density of states and its transformation indicate that the magnitudes of these two quantities are comparable,<sup>6</sup> which argues that coefficients  $A$  and  $C$  should also be close. However, this conclusion relies on the assumption that the matrix elements in Eq. (3) are independent of energy, which may not be valid for the TO phonons in GaN. A theoretical study of the real and imaginary parts of phonon self-energies in zinc blende semiconductors describes situations where the shift and broadening functions differ significantly for TO phonons, notably for GaP.<sup>15</sup> However, this effect is correlated with an asymmetric Raman line shape in GaP, which is not observed in our measurements of the GaN TO phonons.

The lifetimes of the Raman active GaN phonons studied here are obtained using Eq. (1) and the measured linewidths. The  $A_1(\text{TO})$  and  $E_1(\text{TO})$  phonons have low-temperature lifetimes of 0.91 and 1.55 ps, respectively. These values are close to the  $\sim 0.8$  ps lifetime calculated from published Raman linewidths.<sup>12</sup> The longer  $E_2^2$  lifetime,  $\sim 3.0$  ps, is attributed to the inefficient three-phonon decay process.

### V. $A_1(\text{LO})$ AND $E_1(\text{LO})$ PHONON DECAY

Turning our attention to the LO phonons, we analyze the temperature dependence of our  $A_1(\text{LO})$  data, as shown in Fig. 5. In this case, we find that both two- and three-phonon decay processes are necessary to adequately describe the dependences. The asymmetrical two-phonon decay plays a larger role than the symmetrical three-phonon mechanism in

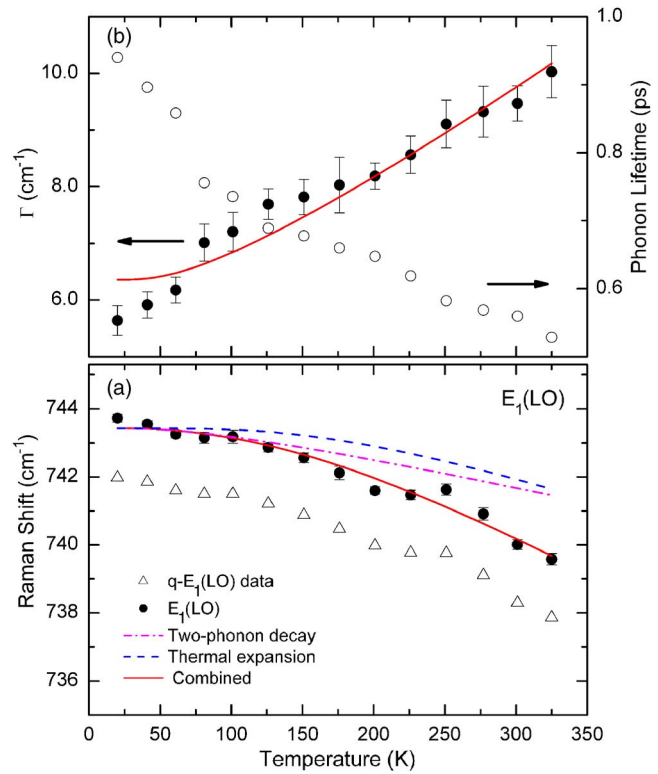


FIG. 6. (Color online) Dependence of  $E_1(\text{LO})$  phonon energies (a) and linewidths (b) on temperature, similar to Fig. 2.

the  $A_1(\text{LO})$  phonon temperature dependence. The two-phonon process creates phonons with energies of 559 and 180  $\text{cm}^{-1}$ . An examination of phonon dispersion curves<sup>23,24</sup> suggests that the two decay processes  $A_1(\text{LO}) \rightarrow E_1(\text{TO}) + E_2^1$  and  $A_1(\text{LO}) \rightarrow E_1(\text{TO}) + \text{TA}(\text{LA})$  from the  $L$  point of the Brillouin zone would satisfy the conservations of energy and wave vector. Our results are consistent with the Ridley process.<sup>8</sup> The individual curves in Fig. 5(a) show that the contribution from two-phonon decay is comparable to that of thermal expansion and is larger than what we attribute to three-phonon decay. This decay assignment agrees well with prior reports for the  $A_1(\text{LO})$  band.<sup>10,11</sup>

$A_1(\text{TO})$  and  $E_1(\text{TO})$  phonon modes are dominant when GaN Raman spectra are taken in a backscattering geometry from the cross section of the epilayer, and a weak scattering from the forbidden quasi- $E_1(\text{LO})$  [ $q-E_1(\text{LO})$ ] phonon is also observed (Fig. 1). When the backscattering is not strictly parallel or perpendicular to an optical axis of the wurtzite structure of GaN,  $A_1(\text{LO})$  and  $E_1(\text{LO})$  modes may mix to produce a quasi- $E_1(\text{LO})$  mode.<sup>25</sup> The frequency of the  $q-E_1(\text{LO})$  is defined in terms of the pure  $A_1(\text{LO})$  and  $E_1(\text{LO})$  modes as<sup>26</sup>

$$\omega_{q-E_1(\text{LO})}^2 = \omega_{A_1(\text{LO})}^2 \cos^2 \theta + \omega_{E_1(\text{LO})}^2 \sin^2 \theta, \quad (7)$$

where  $\theta$  is the angle between the  $c$  axis and the phonon propagation direction. Using the method of Ref. 26, and their room-temperature  $E_1(\text{LO})$  value along with our measured  $A_1(\text{LO})$  and quasi- $E_1(\text{LO})$  energies, we determine the values of  $E_1(\text{LO})$  from  $T=20$ – $325$  K. Raw data for the  $q-E_1(\text{LO})$  and the obtained  $E_1(\text{LO})$  are shown in Fig. 6.

As with the other phonons discussed above, we analyze  $\omega$  and  $\Gamma$  for the  $E_1(\text{LO})$  line using Eqs. (5) and (6). Because they exhibit the same temperature dependence,<sup>25</sup> fitting the raw  $E_1(\text{LO})$  data gives the same decay picture as the analysis of  $q\text{-}E_1(\text{LO})$ . The  $E_1(\text{LO})$  phonon exhibits asymmetric decay, producing phonons with energies of 605 and 140  $\text{cm}^{-1}$ . The dispersion curves<sup>23,24</sup> reveal the decay process  $E_1(\text{LO}) \rightarrow E_2^2 + \text{LA}(\text{TA})$ , where the created vibrations are from the high density of state  $M$  point region of the Brillouin zone. Similar to the  $A_1(\text{LO})$  phonon, the contribution from the two-phonon decay process is comparable in magnitude to that from thermal expansion.

We find that the relative two-phonon decay probabilities ( $A$  and  $C$ ) obtained from energy shift and linewidth broadening are comparable for  $A_1(\text{LO})$  and  $E_1(\text{LO})$ . For the  $A_1(\text{LO})$  phonon, we likewise see that the three-phonon decay parameters  $B$  and  $D$  are consistent. The agreement between coefficients  $A$  and  $C$  ( $B$  and  $D$ ) is expected when decay is related to a small set of dominant channels and when  $|V_3|^2$  ( $|V_4|^2$ ) is largely independent of energy in carrying out the Kramers-Kronig transformation in Eq. (4) Ref. 6 along with the approximations made in arriving at Eqs. (5) and (6).

The  $T \rightarrow 0$  lifetimes of GaN  $A_1(\text{LO})$  and  $E_1(\text{LO})$  phonons are 1.44 and 0.94 ps, respectively. The  $A_1(\text{LO})$  phonon lifetime compares well with measurements using time-resolved spectroscopy.<sup>27</sup> Published results for the  $A_1(\text{LO})$  phonon lifetime in AlN are  $\sim 0.8$  ps<sup>5,20</sup> in agreement with our value for GaN. This is attributed to the consistency of the decay mechanism in the two materials due to similar phonon dispersion curves.

## VI. SUMMARY

In agreement with previously published work,<sup>10,11</sup> we find the  $A_1(\text{LO})$  vibration primarily decays via Ridley two-phonon creation with a weak contribution from three-phonon creation. The  $E_1(\text{LO})$  phonon, which has received little attention, exhibits two-phonon asymmetric (Ridley) decay without the need of a higher-order term. For each of these LO phonons, the relative two-phonon probabilities ( $A$  and  $C$ ) obtained from energy shift and linewidth broadening are comparable. Furthermore, the  $A$  and  $C$  values also compare well between the  $A_1(\text{LO})$  and  $E_1(\text{LO})$  phonons. This agreement strongly supports the similarities concluded regarding the LO phonon decay properties. For the  $A_1(\text{LO})$  phonon, the three-phonon decay parameters  $B$  and  $D$  are also consistent.

The  $A_1(\text{TO})$  and  $E_1(\text{TO})$  phonons both decay symmetrically into vibrations from the high density of state regions in the 200–300  $\text{cm}^{-1}$  range. In contrast to the LO phonons, the two-phonon decay coefficients  $A$  obtained from the energy

shift are much smaller than the  $C$  coefficients obtained from linewidth broadening for both GaN TO phonons. It would be interesting to compare our results concerning decay coefficients with similar studies of AlN and InN to explore how general the decay processes are in this family of materials. *Ab initio* theory concerning the nitride semiconductors would clearly be useful in interpreting the results since the matrix elements in Eq. (3) can also be addressed to see how much of the disparity between  $A$  and  $C$  can be attributed to these factors.

## ACKNOWLEDGMENTS

The authors acknowledge support for this work by the National Science Foundation (ECS-0609416 and ECS-0304224) and the J. F. Maddox Foundation.

- <sup>1</sup>S. A. Vitusevich *et al.*, Appl. Phys. Lett. **82**, 748 (2003).
- <sup>2</sup>I. Ahmad, V. Kasisomayajula, M. Holtz, J. M. Berg, S. R. Kurtz, C. P. Tigges, A. A. Allerman, and A. G. Baca, Appl. Phys. Lett. **86**, 173503 (2005).
- <sup>3</sup>V. O. Turin and A. A. Balandin, J. Appl. Phys. **100**, 054501 (2006).
- <sup>4</sup>A. J. Kent and J. K. Wigmore, in *Electron-Phonon Interactions in Low-Dimensional Structures*, Edited by L. Challis (Oxford University Press, Oxford, 2003), Chap. 2.
- <sup>5</sup>M. Kuball, J. M. Hayes, Y. Shi, and J. H. Edgar, Appl. Phys. Lett. **77**, 1958 (2000).
- <sup>6</sup>M. Giehler, M. Ramsteiner, P. Waltreit, O. Brandt, K. H. Ploog, and H. Obloh, J. Appl. Phys. **89**, 3634 (2001).
- <sup>7</sup>P. G. Klemens, Phys. Rev. **148**, 845 (1966).
- <sup>8</sup>B. K. Ridley, J. Phys.: Condens. Matter **8**, L511 (1996).
- <sup>9</sup>A. Link *et al.*, J. Appl. Phys. **86**, 6256 (1999).
- <sup>10</sup>X. B. Chen, J. Huso, J. L. Morrison, L. Bergman, and A. P. Purdy, J. Appl. Phys. **98**, 026106 (2005).
- <sup>11</sup>D. Y. Song, M. Basavaraj, S. Nikishin, M. Holtz, V. Soukhoveev, A. Usikov, and V. Dmitriev, J. Appl. Phys. **100**, 113504 (2006).
- <sup>12</sup>W. S. Li, Z. X. Shen, Z. C. Feng, and S. J. Chua, J. Appl. Phys. **87**, 3332 (2000).
- <sup>13</sup>J. Menendez and M. Cardona, Phys. Rev. B **29**, 2051 (1984).
- <sup>14</sup>A. Debernardi, Phys. Rev. B **57**, 12847 (1998).
- <sup>15</sup>A. Debernardi, Solid State Commun. **113**, 1 (2000).
- <sup>16</sup>M. Balkanski, R. F. Wallis, and E. Haro, Phys. Rev. B **28**, 1928 (1983).
- <sup>17</sup>J. J. Sakurai, *Modern Quantum Mechanics* (Addison-Wesley, Reading, MA, 1994).
- <sup>18</sup>M. Cardona and T. Ruf, Solid State Commun. **117**, 201 (2001).
- <sup>19</sup>G. Deinzer, M. Schmitt, A. P. Mayer, and D. Strauch, Phys. Rev. B **69**, 014304 (2004).
- <sup>20</sup>D. Y. Song, M. Holtz, A. Chandolu, S. A. Nikishin, E. N. Mokhov, Y. Makarov, and H. Helava, Appl. Phys. Lett. **89**, 021901 (2006).
- <sup>21</sup>R. R. Reeber and K. Wang, J. Mater. Res. **15**, 40 (2000).
- <sup>22</sup>M. Holtz, M. Seon, T. Prokofyeva, H. Temkin, R. Singh, F. P. Dabkowski, and T. D. Moustakas, Appl. Phys. Lett. **75**, 1757 (1999).
- <sup>23</sup>T. Ruf *et al.*, Phys. Rev. Lett. **86**, 906 (2001).
- <sup>24</sup>V. Yu. Davydov *et al.*, Phys. Rev. B **58**, 12899 (1998).
- <sup>25</sup>H. Harima, J. Phys.: Condens. Matter **14**, R967 (2002).
- <sup>26</sup>K. Torii, M. Ono, T. Sota, T. Azuhata, S. F. Chichibu, and S. Nakamura, Phys. Rev. B **62**, 10861 (2000).
- <sup>27</sup>K. T. Tsen, D. K. Ferry, A. Botchkarev, B. Sverdlov, A. Salvador, and H. Morkoc, Appl. Phys. Lett. **72**, 2132 (1998).